Received: Added at production | Revised: Added at production | Accepted: Added at production
DOI: xxx/xxxx

ARTICLE TYPE

Integral Sliding Mode-Based Event-Triggered Nearly Optimal Tracking Control for Uncertain Nonlinear Systems

Shunchao Zhang[1] | Yonghua Wang[2] | Dacai Liu[1] | Jiawei Zhuang[2] | Yongwei Zhang*[2]

[1]School of Internet Finance and Information Engineering, Guangdong University of Finance, Guangzhou 510521, China
[2]School of Automation, Guangdong University of Technology, Guangzhou 510006, China

Correspondence
*Yongwei Zhang. School of Automation, Guangdong University of Technology, Guangzhou 510006, China. Email: Yongwei_Zhang@mail2.gdut.edu.cn

Summary

In this paper, an event-triggered nearly optimal tracking control method is investigated for a class of uncertain nonlinear systems by integrating adaptive dynamic programming (ADP) and integral sliding mode (ISM) control. By introducing a neural network (NN) adaptive term, the designed ISM-based discontinuous control law is employed to eliminate the influence of the uncertainties and obtain the tracking error system constructed from the sliding mode dynamics, as well as relax the known upper-bounded condition of uncertainties. In order to guarantee the stability of tracking error system and improve the control performance, under the ADP technique, a critic NN is applied to approximate the optimal value function for solving the event-triggered Hamilton-Jacobi-Bellman equation and the event-triggered nearly optimal feedback control is obtained. The feedback control law is updated and transmitted to plant only when events occur, thus both the communication and the computational resources can be saved. Furthermore, the stability of tracking error is proven thanks to Lyapunov's direct method. Finally, we provide two simulation examples to validate the developed control scheme.

KEYWORDS:
Integral sliding mode control, adaptive dynamic programming, neural networks, event-triggered mechanism, uncertain systems.

1 | INTRODUCTION

With the existing of model uncertainties and disturbance, there will always be a deviation between practical control systems and their nominal systems employed for controllers design.[1,2] It is necessary to investigate a robust control method for guaranteeing the stability and desired performance of systems in the presence of deviation. During the past few years, many advanced control methods, such as adaptive control,[3,4] robust control,[5] H_∞ control,[6] and sliding mode control (SMC),[7,8] have been used to design robust controller. Among these methods, as an effective technique, SMC has widely employed in solving the robust control problem due to the insensitive of parameter changes and the ability of fast respond.[9,10,11,12] Liu et al.[11] proposed an adaptive SMC method for nonlinear systems with parametric uncertainties and external disturbances by combining immersion and invariance adaptive scheme. Ding et al.[12] developed a discontinuous and a quasi-continuous second-SMC methods for uncertain nonlinear systems, and the chattering phenomenon was reduced in the last method to some extent. The traditional SMC composes two parts, i.e., the initial reaching phase and the sliding motion phase, and the robustness is only occurred during the sliding motion. In order to avoid the reaching phase and improve the robustness, many integral SMC (ISMC) methods[13,14,15] have been developed in recent years. Cao et al.[13] developed an ISMC method for nonlinear systems with uncertainties by designing a nonlinear integral-type sliding mode surface (SMS). In these methods, the system trajectory starts on the sliding manifold for any initial system state by designing an integral sliding mode function.

Although the aforementioned methods have been widely employed to design robust controllers, which are not only required to stabilize the systems with uncertainties, but also satisfy the considerable optimality in practical applications.[16] By integrating ISMC technique and optimal control (OC) approaches, many approaches designed a composite control law to achieve the objective for linear systems.[17,18,19,20,21,22] Surjagade et al.[21] developed an optimal ISMC method for a pressurized heavy water reactor system, this method combined the optimal control law with ISMC law to guarantee the stability of the closed-loop system when the existing of uncertainties and external disturbances. Das and Mahanta[22] proposed an optimal second-order SMC method for uncertain linear systems by combining the terminal SMS and the integral SMS. On the whole, in the these methods, a discontinuous control law is employed to eliminate the effect of uncertainties or disturbances and obtain sliding mode dynamics, and the OC law from solving algebraic Riccati equation is obtained to stabilize the linear sliding mode dynamics. However, for the nonlinear systems, these methods are not easy to implement since they are difficult to design the OC law for the nonlinear sliding mode dynamics by solving Hamilton-Jacobi-Bellman (HJB) equation, which is difficult or even impossible to obtain the analysis solution.

Fortunately, adaptive dynamic programming (ADP) and reinforcement learning (RL) which are viewed as synonyms are two effective techniques developed to overcome this difficulty by computing forward-in-time[23,24,25]. Many significant ADP-based control methods have been reported to solve the OC problem for nonlinear systems[26,27]. Vamvoudakis and Lewis[28] developed an actor-critic (AC) strategy to solve the OC problem for nonlinear systems. Vrabie and Lewis[29] developed an integral RL method to obtain the solution of HJB equation and solve the OC problem of partially known nonlinear systems. It is easy to find that the aforementioned results are achieved for optimal regulation problems. However, in many practical systems, the objective of controller design is to guarantee the system state tracking an user-defined reference trajectory rather than regulate the system state approaching the origin. Hence, it is significant to track the user-defined reference trajectory with optimal performance and is also one of the common problem in ADP- or RL-based control community. For discrete-time (DT) nonlinear systems, the optimal tracking control problem was converted into an OC problem for tracking error dynamics and a neuro-optimal tracking control scheme was developed for nonlinear systems via the ADP technique.[32] Wei et al.[33] developed a data-based optimal tracking control method for DT nonlinear systems and to apply the coal gasification system. For continuous-time (CT) nonlinear systems, Modares and Lewis[34] developed an integral RL-based tracking control method for CT nonlinear systems. Zhao et al.[35] developed an ADP-based robust tracking control method for CT nonlinear systems with uncertainties, where the tracking control problem was transformed into an OC problem for the augmented system. Wang et al.[36] developed an adaptive-critic-based robust tracking control method for uncertain nonlinear systems, and this method was applying to a spring-mass-damper system.

However, these methods adopted time-triggered mechanism, the updating of the control law with a fixed period may increase the energy consumption, and waste computational and communication resources. In order to save the computational and communication resources on the basis of satisfying some control performance, many researchers have introduced event-triggered mechanism to ADP, and developed many ADP-based ETC methods,[37,38,39,40] where the event was defined as the event-triggering error exceeded the designed event-triggering condition and the control law was updated only when the occurrence of the events. For example, Vamvoudakis[39] developed an event-triggered OC (ETOC) method for CT nonlinear systems, this method was implemented based on AC structure, a critic and an actor neural networks (NNs) were employed to approximate the cost function and the ETOC law, respectively. Wang et al.[40] developed an event-triggered robust control method for uncertain CT nonlinear systems, where the robust control problem was transformed into an ETOC problem by designed a modified value function. For the tracking control problem, Zhang et al.[41] developed an event-triggered tracking control (ETTC) scheme for CT nonlinear systems, the designed control law composited with a feedforward and a feedback control laws which were employed to track the reference trajectory and stabilize tracking error dynamics, respectively.

Based on the above-mentioned literature, these methods involved precise system dynamics only, research in ADP-based ETTC has not been fully taken into account. However, the uncertainties is widely existed between actual plant and its nominal system. On the other hand, among existing methods[35,40,41,42] required the upper-bounded function of the uncertainties which is difficult to be obtained. Inspired by the aforementioned literature, this paper focus on developing an event-triggered nearly optimal tracking control (ETNOTC) method for uncertain nonlinear systems by integrating ADP and ISMC. The main contributions of this scheme is summarized in the following three aspects.

1. In contrast to existing methods[17,18,19,21,20,22] which proposed ISMC methods integrated with OC approaches for uncertain linear systems, this paper develops an ETNOTC method based on ADP technique for uncertain nonlinear systems.

2. Unlike works[35,40,41,42] required the assumption that the known upper bound of the uncertainties, this paper adopts the ISMC technique with an adaptive term to eliminate the effect of uncertainties and relax the assumption simultaneously.
3. Different from works[17,18,19,21,20,22,30,31] which adopted time-triggered mechanism to design the nearly optimal continuous control law, this paper develops an ETC method to save the computational and communication resources.

The reminder of this paper is organized as follows. Section 2 presents the problem statement. Section 3 introduces the composite control law design in detail. In Section 4, a numerical and a practical examples are employed to verify the effectiveness of ETNOTC method. In Section 5, conclusion is given.

2 | PROBLEM STATEMENT

Consider the uncertain nonlinear system described by

$$\dot{s}(t) = \mathcal{F}\big(s(t)\big) + \mathcal{G}\big(s(t)\big)u(t) - \Delta\mathcal{F}\big(s(t)\big), \tag{1}$$

where $s \in \mathbb{R}^n$ and $u \in \mathbb{R}^m$ are the system state and the control input, respectively, $\Delta\mathcal{F}(s) = \mathcal{G}(s)d(s) \in \mathbb{R}^n$ is the uncertain term, $\mathcal{F}(s) \in \mathbb{R}^n$ and $\mathcal{G}(s) \in \mathbb{R}^{n\times m}$ are continuously differentiable matrix functions, and $\mathcal{G}(s)$ is invertible.

Assumption 1. The system (1) is controllable, and the system dynamic $\mathcal{F}(s) + \mathcal{G}(s)u$ is Lipschitz continuous on a compact set Ω and $\mathcal{F}(0) = 0$.

For the tracking control, the system state is expected to track an user-defined reference trajectory which is give by

$$\dot{x}_d(t) = \phi(x_d), \tag{2}$$

where $x_d \in \mathbb{R}^n$ is the reference state, and $\phi(x_d) \in \mathbb{R}^n$ is an Lipschitz continuous function. According to (1) and (2), the tracking error is defined as $\delta(t) = s(t) - x_d(t)$. Then, the tracking error system can be described as

$$\begin{aligned}\dot{\delta}(t) &= \dot{s}(t) - \dot{x}_d(t)\\ &= \mathcal{F}(s) + \mathcal{G}(s)u(t) - \Delta\mathcal{F}(s) - \phi(x_d).\end{aligned} \tag{3}$$

In the following, a composite control law u is designed to guarantee the system state tracking the reference trajectory and minimize a given value function as far as possible.

3 | COMPOSITE CONTROL LAW DESIGN VIA ISMC AND ADP

For the tracking error system (3), an ETNOTC method which integrates ADP and ISMC techniques is developed to design a composite control law as

$$u = u_c + u_d + w, \tag{4}$$

where $u_c \in \mathbb{R}^m$ is the discontinuous component to eliminate the influence of the uncertainties, $u_d \in \mathbb{R}^m$ is the continuous feedforward control component to track the trajectory, $w \in \mathbb{R}^m$ is the continuous ADP-based feedback control component to guarantee the tracking error stabilization.

3.1 | Discontinuous control law design via ISMC

The integral sliding mode (ISM) function is designed as

$$S(\delta(t), t) = A\delta - A\delta_0 - \int_0^t A\Big(\mathcal{F}\big(s(\tau)\big) + \mathcal{G}\big(s(\tau)\big)W(\tau) - \phi(x_d)\Big)d\tau, \tag{5}$$

where $\delta_0 = s(0)$, $W = u_d + w$, $A \in \mathbb{R}^{m\times n}$ is a design matrix. It is worth pointing out that the ISM function satisfies $S(\delta_0, t) = 0$, the system state starts on the ISM surface, thus the reaching phase can be removed.

Differentiating $S(\delta(t), t)$ with respect to t, it yields

$$\begin{aligned}\dot{S}(\delta, t) &= A\dot{\delta} - A\big(\mathcal{F}(s) + \mathcal{G}W - \phi(x_d)\big)\\ &= A\big(\mathcal{F}(s) + \mathcal{G}(s)(u - d(s)) - \phi(x_d)\big) - A\big(\mathcal{F}(s) + \mathcal{G}(s)W - \phi(x_d)\big)\\ &= A\mathcal{G}(s)\big(u_c - d(s)\big).\end{aligned}$$

According to SMC theory, let $\dot{S}(s, t) = 0$, the equivalent control law u_{ceq} is derived as

$$u_{ceq} = d(s). \tag{6}$$

Substituting (6) into (3), we get the sliding mode dynamics as

$$\dot{\delta}(t) = \mathcal{F}(s) + \mathcal{G}(s)W - \phi(x_d). \tag{7}$$

However, the u_{ceq} cannot be obtained since the unknown $d(s)$. To keep the integral sliding mode function as zero, i.e., $S(\delta, t) = 0$, the discontinuous control law u_c is designed as

$$u_c = -\mathcal{K}\mathrm{sgn}(\Xi), \tag{8}$$

where $\Xi = \mathcal{G}^{\mathsf{T}}(s)A^{\mathsf{T}}S$, $\mathrm{sgn}(\cdot)$ is the sign function, $\mathcal{K} > \bar{d}$ is a sliding mode gain, $\bar{d}$ is the norm-bound of $d(s)$. In order to relax the requirement of the known $\bar{d}$, a radial basis function (RBF) NN-based adaptive team is designed to estimate the uncertainties as

$$d(s) = \theta^{*\mathsf{T}}h(s) + \epsilon,$$

where $\theta^* \in \mathbb{R}^{l_d\times m}$ is the ideal weight, l_d is the number of neurons, $h(s) \in \mathbb{R}^{l_d}$ is a RBF, and ϵ is the approximation error. Denote $\hat{\theta} \in \mathbb{R}^{l_d\times m}$ be the estimation of θ^*, we have

$$\hat{d}(s) = \hat{\theta}^{\mathsf{T}}h(s).$$

Furthermore, the discontinuous control law u_c in (8) is changed as

$$u_c = -K\mathrm{sgn}(\Xi) + \hat{d}(s), \tag{9}$$

where K is the improved sliding mode gain satisfying $K > \epsilon_b$ and ϵ_b is the norm-bound of ϵ.

Theorem 1. For the nonlinear system (1), the designed integral sliding mode function (5), and Assumption 1, the discontinuous control law u_c (9) can maintain the system state trajectory on the ISM surface $S = 0$ with the adaptive law

$$\dot{\hat{\theta}} = -\frac{1}{\gamma}h(s)S^{\mathsf{T}}A\mathcal{G}(s), \tag{10}$$

where $\gamma > 0$ is the updating rate.

Proof. Consider the Lyapunov function candidate given as

$$\Sigma_1(t) = \frac{1}{2}S^{\mathsf{T}}S + \frac{\gamma}{2}\mathrm{tr}\{\tilde{\theta}^{\mathsf{T}}\tilde{\theta}\}, \tag{11}$$

where $\tilde{\theta} = \hat{\theta} - \theta^*$. The time derivative of the Σ_1 is deduced as

$$\begin{aligned}\dot{\Sigma}_1(t) &= S^{\mathsf{T}}A\Big(\mathcal{F}(s) + \mathcal{G}(s)\big(u - d(s)\big) - \phi(x_d)\Big) - S^{\mathsf{T}}A\big(\mathcal{F}(s) + \mathcal{G}(s)W - \phi(x_d)\big) + \gamma\mathrm{tr}\{\tilde{\theta}^{\mathsf{T}}\dot{\tilde{\theta}}\}\\ &= S^{\mathsf{T}}A\Big(\mathcal{F}(s) + \mathcal{G}(s)\big(u_c + W - d(s)\big)\Big) - S^{\mathsf{T}}A(s)\big(\mathcal{F}(s) + \mathcal{G}(s)W\big) + \gamma\mathrm{tr}\{\tilde{\theta}^{\mathsf{T}}\dot{\tilde{\theta}}\}\\ &= S^{\mathsf{T}}A\Big(\mathcal{G}(s)\big(-K\mathrm{sgn}(\Xi) + \hat{d}(s) - d(s)\big)\Big) + \gamma\mathrm{tr}\{\tilde{\theta}^{\mathsf{T}}\dot{\tilde{\theta}}\}\\ &= -KS^{\mathsf{T}}A\mathcal{G}(s)\mathrm{sgn}(\Xi) + \gamma\mathrm{tr}\{\tilde{\theta}^{\mathsf{T}}\dot{\tilde{\theta}}\} + S^{\mathsf{T}}A(s)\mathcal{G}(s)\big(\hat{d}(s) - d(s)\big)\\ &= -KS^{\mathsf{T}}A\mathcal{G}(s)\mathrm{sgn}(\Xi) + \gamma\mathrm{tr}\{\tilde{\theta}^{\mathsf{T}}\dot{\tilde{\theta}}\} + S^{\mathsf{T}}A\mathcal{G}(s)\big(\hat{\theta}^{\mathsf{T}}h(s) - \theta^{*\mathsf{T}}h(s) - \epsilon\big).\end{aligned} \tag{12}$$

Considering the adaptive law (10) and $\dot{\tilde{\theta}} = \dot{\hat{\theta}}$, (12) becomes

$$\begin{aligned}\dot{\Sigma}_1(t) &= -KS^{\mathsf{T}}A\mathcal{G}(s)\mathrm{sgn}(\Xi) + S^{\mathsf{T}}A\mathcal{G}(s)\big(\tilde{\theta}^{\mathsf{T}}h(s) - \epsilon\big) - \mathrm{tr}\{\tilde{\theta}^{\mathsf{T}}h(s)S^{\mathsf{T}}A\mathcal{G}(s)\}\\ &= -KS^{\mathsf{T}}A\mathcal{G}(s)\mathrm{sgn}(\Xi) - S^{\mathsf{T}}A\mathcal{G}(s)\epsilon\\ &\leq -K\|S^{\mathsf{T}}A\mathcal{G}(s)\|_1 - \|S^{\mathsf{T}}A\mathcal{G}(s)\epsilon\|\end{aligned}$$

$$\leq -(K-\epsilon_b)\|S^{\mathsf{T}}A\mathcal{G}(s)\|_1. \tag{13}$$

Therefore, if $K > \epsilon_b$ holds, the system state trajectory is maintained on sliding mode surface. □

Remark 1. It is noticed that the improved sliding mode gain K is different from the gain $\mathcal{K}$ and depends on the norm-bound of approximation error ϵ instead of the norm-bound of the uncertain term $d(s)$. In practical applications, it is difficult to obtain the norm-bound of of the uncertain term. The approximation error ϵ can be guaranteed to be arbitrary small by selecting sufficient number of neurons.[43,44] Although the selection of gain K is challenging, there is no guiding method to select an optimal sliding mode gain, and it can be selected based on repeated "trial and error".

Remark 2. It is evident from (13) if the sliding mode gain K is chosen as $K > \epsilon_b$, we have $\dot{\Sigma}_1(t) =$ the Lyapunov candidate function (11) will decrease gradually and the sliding mode surface S will converge to zero in finite time.

3.2 | Continuous control law design via ADP

Assume that the desired trajectory satisfies

$$\dot{x}_d(t) = \mathcal{F}(x_d) + \mathcal{G}(x_d)u_d, \tag{14}$$

where u_d is the feedforward control law. Combining (2) and (14), we have

$$u_d = \mathcal{G}^{+}(x_d)\big(\phi(x_d) - \mathcal{F}(x_d)\big), \tag{15}$$

where $\mathcal{G}^{+}(x_d)$ denotes the generalized inverse of $\mathcal{G}(x_d)$. Substituting (15) into (7), the tracking error dynamics is given by

$$\begin{aligned}\dot{\delta}(t) &= \dot{x}(t) - \dot{x}_d(t)\\ &= \mathcal{F}(s) + \mathcal{G}(s)(u_d + w) - \phi(x_d)\\ &= \mathcal{F}(s) + \mathcal{G}(s)\mathcal{G}^{+}(x_d)\big(\phi(x_d) - \mathcal{F}(x_d)\big) + \mathcal{G}(s)w - \phi(x_d).\end{aligned}$$

Letting $\mathcal{F}_\delta = \mathcal{F}(s) + \mathcal{G}(s)\mathcal{G}^{+}(x_d)\big(\phi(x_d) - \mathcal{F}(x_d)\big) - \phi(x_d)$, we have

$$\dot{\delta}(t) = \mathcal{F}_\delta + \mathcal{G}(s)w. \tag{16}$$

Then, under the event-triggered mechanism, an ADP-based control method is developed to design the feedback control law w. The value function of (16) is defined as

$$V(\delta) = \int_t^{\infty} \Big(\delta^{\mathsf{T}}(\tau)Q_\delta\delta(\tau) + w^{\mathsf{T}}(\tau)Rw(\tau)\Big)d\tau, \tag{17}$$

where $Q_\delta \in \mathbb{R}^{n\times n}$ and $R \in \mathbb{R}^{m\times m}$ are symmetric positive definite matrices. Based on (17), we have

$$0 = \delta^{\mathsf{T}}Q_\delta\delta + w^{\mathsf{T}}Rw + \nabla V^{\mathsf{T}}(\delta)\big(\mathcal{F}_\delta + \mathcal{G}(s)w\big)$$

with $V(0) = 0$, where $\nabla V(\delta) \triangleq \partial V(\delta)/\partial\delta$. The Hamiltonian of system (16) is given by

$$H(\nabla V(\delta), \delta, w) = \delta^{\mathsf{T}}Q_\delta\delta + w^{\mathsf{T}}Rw + \nabla V^{\mathsf{T}}(\delta)\big(\mathcal{F}_\delta + \mathcal{G}(s)w\big).$$

The optimal value function $V^*(\delta)$ satisfy the following HJB equation

$$0 = \min_w H(\nabla V^*(\delta), \delta, w), \tag{18}$$

where $\nabla V^*(\delta) \triangleq \partial V^*(\delta)/\partial\delta$. We drive from (18) that

$$\left.\frac{\partial H\big(\delta, \nabla V^*(\delta), w\big)}{\partial w}\right|_{w=w^*} = 0,$$

where w^* is the optimal tracking control law and given by

$$w^*(\delta) = -\frac{1}{2}R^{-1}\mathcal{G}^{\mathsf{T}}(\delta)\nabla V^*(\delta). \tag{19}$$

Substituting (19) into (18), we further obtain

$$H(\nabla V_i^*(\delta), \delta, w^*) = \delta^{\mathsf{T}}Q_\delta\delta + w^{*\mathsf{T}}Rw^* + \nabla V^{*\mathsf{T}}(\delta)\big(\mathcal{F}_\delta + \mathcal{G}(s)w^*\big)$$

$$= 0. \tag{20}$$

From (20), it is a time-triggered HJB equation whose solution often involves heavy computational burden and the waste of communication resource by using ADP-based time-triggered mechanism. Hence, we developed an ADP-based ETC method to obviate this shortcoming. Under the ETC framework, the sampled state is denoted as

$$\hat{s}_\kappa = s(t_s), \quad \forall t \in [t_\kappa, t_{\kappa+1}),$$

where t_κ represents the κth sampling instant, $\kappa \in \mathbb{N}$. The corresponding tracking error is given by

$$\hat{\delta}_\kappa = \hat{s}_\kappa - x_d(t_\kappa), \quad \forall t \in [t_\kappa, t_{\kappa+1}).$$

Then, introduce an triggering error function as

$$\mathbf{E}_\kappa(t) = \hat{\delta}_\kappa - \delta(t), \quad \forall t \in [t_\kappa, t_{\kappa+1}). \tag{21}$$

According to (21), the ETC law is expressed by

$$w(\hat{\delta}_\kappa) = w\big(\mathbf{E}_\kappa(t) + \delta(t)\big), \tag{22}$$

Based on (22), the system (16) becomes

$$\dot{\delta}(t) = \mathcal{F}_\delta + \mathcal{G}(s)w(\hat{\delta}_\kappa). \tag{23}$$

Furthermore, the event-triggered optimal tracking control (ETOTC) can be obtained from (23) as

$$w^*(\hat{\delta}_s) = -\frac{1}{2}R^{-1}\mathcal{G}^\mathsf{T}(\hat{\delta}_\kappa)\nabla V^*(\hat{\delta}_\kappa) \tag{24}$$

for all $t \in [t_\kappa, t_{\kappa+1})$, where $\nabla V^*(\hat{\delta}_\kappa) \triangleq \partial V^*(\hat{\delta}_\kappa)/\partial\hat{\delta}_\kappa$. By replacing w in (18) with $w^*(\hat{\delta}_s)$, the event-triggered version of HJB equation at $t = t_\kappa$ is written as

$$H\big(\nabla V^*(\delta), \delta, w^*(\hat{\delta}_\kappa)\big) = \delta^\mathsf{T} Q_\delta \delta + w^{*\mathsf{T}}(\hat{\delta}_\kappa)Rw^*(\hat{\delta}_\kappa) + \nabla V^{*\mathsf{T}}(\delta)\big(\mathcal{F}_\delta + \mathcal{G}(s)w^*(\hat{\delta}_\kappa)\big).$$

Assumption 2. $w^*(\delta)$ is Lipschitz continuous, i.e., $\|w^*(\delta(t)) - w^*(\hat{\delta}_\kappa)\| \leq \mathcal{L}_w\|\mathbf{E}_\kappa(t)\|$, where $\mathcal{L}_{wi} > 0$ is a constant.

Theorem 2. For the tracking error system given by (3), the sliding mode dynamics (16), Assumptions 1–2, the composite control law (4) with (9), (15) and (24), if the triggering condition is designed as

$$\|\mathbf{E}_\kappa\|^2 \leq \frac{(1-\beta^2)\delta^\mathsf{T} Q_\delta \delta + \|r\|^2\|w^*(\hat{\delta}_\kappa)\|^2}{\mathcal{L}_w^2} = T_\kappa^2, \tag{25}$$

where $\mathcal{L}_w$ is a positive constant, T_κ is the event-triggering threshold, the closed-loop tracking error system (3) is guaranteed to be asymptotically stable.

Proof. Choose a Lyapnuov function candidate as

$$\Sigma_2(t) = V^*(\delta).$$

Based on Theorem 1, by using the discontinuous control law u_c, the system state trajectory can be forced on integral sliding mode surface $S = 0$ and maintained on it. And then, applying the feedforward control law, the tracking error system is obtained as (16). Using the trajectories of system (16), we find

$$\dot{\Sigma}_2(t) = \nabla V^{*\mathsf{T}}(\delta)\big(\mathcal{F}_\delta + \mathcal{G}(s)w^*(\hat{\delta}_\kappa)\big). \tag{26}$$

Based on (19), we have

$$\nabla V^{*\mathsf{T}}(\delta)\mathcal{G}(s) = -2w^{*\mathsf{T}}(\delta)R. \tag{27}$$

From (20), it reveals that

$$\nabla V^{*\mathsf{T}}(\delta)\mathcal{F}_\delta = -\delta^\mathsf{T} Q_\delta \delta - w^{*\mathsf{T}}(\delta)Rw^*(\delta) - \nabla V^{*\mathsf{T}}(\delta)\mathcal{G}(s)w^*(\delta). \tag{28}$$

Substituting (27) and (28) into (26), we obtain

$$\begin{aligned}\dot{\Sigma}_2(t) &= -\delta^\mathsf{T} Q_\delta \delta - w^{*\mathsf{T}}(\delta)Rw^*(\delta) - \nabla V^{*\mathsf{T}}(\delta)\mathcal{G}(s)w^*(\delta) + \nabla V^{*\mathsf{T}}(\delta)\mathcal{G}(s)w^*(\hat{\delta}_\kappa) \\ &= -\delta^\mathsf{T} Q_\delta \delta + w^{*\mathsf{T}}(\delta)Rw^*(\delta) - 2w^{*\mathsf{T}}(\delta)Rw^*(\hat{\delta}_\kappa)\end{aligned}$$

$$= -\delta^{\mathsf{T}} Q_\delta \delta + \big(w^*(\delta) - w^*(\hat{\delta}_\kappa)\big)^{\mathsf{T}} R\big(w^*(\delta) - w^*(\hat{\delta}_\kappa)\big) - w^{*\mathsf{T}}(\hat{\delta}_\kappa) R w^*(\hat{\delta}_\kappa).$$

According to Assumption 2, we have

$$\begin{aligned}\dot{\Sigma}_2(t) \leq & -\delta^{\mathsf{T}} Q_\delta \delta + \mathcal{L}_w^2 \|r\|^2 \|\mathbf{E}_\kappa(t)\|^2 - \|r\|^2 \|w^*(\hat{\delta}_\kappa)\|^2 \\ \leq & -\beta^2 \lambda_{\min}(Q_\delta)\|\delta\|^2 + (\beta^2 - 1)\lambda_{\min}(Q_\delta)\|\delta\|^2 + \mathcal{L}_w^2 \|r\|^2 \|\mathbf{E}_\kappa(t)\|^2 - \|r\|^2 \|w^*(\hat{\delta}_\kappa)\|^2,\end{aligned}$$

where $R = r^{\mathsf{T}} r$, $r \in R^{m\times m}$ is a square matrix. Then, if condition (25) holds, we have

$$\dot{\Sigma}_2(t) \leq -\beta^2 \lambda_{\min}(Q_\delta)\|\delta\|^2 < 0$$

for any $\delta \neq 0$, it means the closed-loop tracking error system (3) is asymptotically stable. □

3.3 | Critic-only structure implementation

The optimal value function $V^*(\delta)$ can be represented via a critic NN with l_c hidden neurons as

$$V^*(\delta) = \varphi_c^{\mathsf{T}} \sigma_c(\delta) + \xi_c(\delta), \tag{29}$$

where $\varphi_c \in \mathbb{R}^{l_c}$ is the ideal weight vector, $\sigma_c(\delta) \in \mathbb{R}^{l_c}$ is the activation function, and $\xi_c(\delta)$ is the reconstruction error. Differentiating $V^*(\delta)$ in (29) with respect to δ, it yields

$$\nabla V^*(\delta) = \nabla\sigma_c^{\mathsf{T}}(\delta)\varphi_e + \nabla\xi_c(\delta). \tag{30}$$

According to (19) and (30), we have

$$w^*(\hat{\delta}_\kappa) = -\frac{1}{2} R^{-1} \mathcal{G}^{\mathsf{T}}(s)\Big(\nabla\sigma_c^{\mathsf{T}}(\hat{\delta}_\kappa)\varphi_c + \nabla\xi_c(\hat{\delta}_\kappa)\Big). \tag{31}$$

Letting $\hat{\varphi}_c \in \mathbb{R}^{l_c}$ be the estimate of φ_c, the approximate $V^*(\delta)$ is given by

$$\hat{V}(\delta) = \hat{\varphi}_c^{\mathsf{T}} \sigma_c(\delta),$$

and its partial derivative is given by

$$\nabla\hat{V}(\delta) = \nabla\sigma_c^{\mathsf{T}}(\delta)\hat{\varphi}_c. \tag{32}$$

Based on (31) and (32), the approximate ETOTC law is obtained as

$$\hat{w}(\hat{\delta}_\kappa) = -\frac{1}{2} R^{-1} \mathcal{G}^{\mathsf{T}}(s)\nabla\sigma_c^{\mathsf{T}}(\hat{\delta}_\kappa)\hat{\varphi}_c. \tag{33}$$

Noticing (32), the approximate Hamiltonian is defined as

$$\begin{aligned}H_i(\hat{\varphi}_c, \delta, \hat{w}(\hat{\delta}_\kappa)) &= \delta^{\mathsf{T}} Q_\delta \delta + \hat{w}^{*\mathsf{T}}(\hat{\delta}_\kappa) R \hat{w}^*(\hat{\delta}_\kappa) + \nabla V^{*\mathsf{T}}(\delta)\big(\mathcal{F}_\delta + \mathcal{G}(s)\hat{w}^*(\hat{\delta}_\kappa)\big) \\ &= \mathcal{E}_c.\end{aligned}$$

Obviously, we can obtain

$$\frac{\partial\mathcal{E}_c}{\partial\hat{\varphi}_c} = \nabla\sigma_c(\delta)\Big(\mathcal{F}_\delta + \mathcal{G}(s)\hat{w}(\hat{\delta}_\kappa)\Big) \triangleq \pi,$$

where π is a l_c-dimension column vector. To minimize the objective function $\mathcal{O}_c = (1/2)\mathcal{E}_c^{\mathsf{T}}\mathcal{E}_c$, $\hat{\varphi}_c$ is updated by

$$\dot{\hat{\varphi}}_c = -\alpha_c \frac{1}{(1+\pi^{\mathsf{T}}\pi)^2}\left(\frac{\partial\mathcal{O}_c}{\partial\hat{\varphi}_c}\right) = -\alpha_c \frac{\pi}{(1+\pi^{\mathsf{T}}\pi)^2}\mathcal{E}_c, \tag{34}$$

where $\alpha_c > 0$ is the learning rate.

Let $\tilde{\varphi} = \varphi - \hat{\varphi}$ be the weight error vector, then the weight error dynamics is derived as $\dot{\tilde{\varphi}} = -\dot{\hat{\varphi}}$. According to the existing results,[45,47] the weight error dynamics is guaranteed to be UUB with the updating law (34), and the related proof is omitted here.

3.4 | Stability analysis

Assumption 3. $\nabla\sigma_c(\delta)$, $\nabla\xi_c(\delta)$, $\mathcal{G}(s)$ and $\tilde{\varphi}$ are norm-bounded, i.e., $\|\nabla\sigma_c(\delta)\| \leq \bar{\sigma}_c$, $\|\nabla\xi_c(\delta)\| \leq \bar{\xi}_c$, $\|\mathcal{G}(s)\| \leq \bar{g}$ and $\|\tilde{\varphi}\| \leq \bar{\varphi}$, where $\bar{\sigma}_c$, $\bar{\xi}_c$, $\bar{g}$ and $\bar{\varphi}$ are positive constants.[9,46,47]

Theorem 3. Take the system (16) into account, if Assumptions 1–3 hold and the event-triggering condition is designed as

$$\|\mathcal{E}_{\kappa}(t)\|^2 \leq \frac{(1-\rho^2)\lambda_{\min}(\mathcal{Q}_{\delta})\|\delta\|^2}{2\mathcal{L}_w^2} = \hat{T}_{\kappa}^2, \tag{35}$$

where $0 < \rho < 1$, and $\hat{T}_{\kappa}$ is the event-triggering threshold. Then, the approximate ETOTC law (33) can guarantee the closed-loop system (16) to be UUB.

Proof. Choose a Lyapunov function candidate as

$$\Sigma_3(t) = \Sigma_{31}(t) + \Sigma_{32}(t),$$

where $\Sigma_{31}(t) = V^*(\delta)$ and $\Sigma_{32}(t) = V^*(\hat{\delta}_{\kappa})$. The stability analysis is presented as the following two cases.

Case 1: $\forall t \in [t_{\kappa}, t_{\kappa+1})$, we have

$$\dot{\Sigma}_{32}(t) = 0, \tag{36}$$

According to (20), we can derive

$$\begin{aligned}\dot{\Sigma}_{31}(t) =& -\delta^{\mathsf{T}} Q_{\delta}\delta - w^{*\mathsf{T}}(\delta)Rw^*(\delta) - \nabla V^{*\mathsf{T}}(\delta)\mathcal{G}(s)w^*(\delta) + \nabla V^{*\mathsf{T}}(\delta)\mathcal{G}(s)\hat{w}(\hat{\delta}_{\kappa})\\ =& -\delta^{\mathsf{T}} Q_{\delta}\delta - w^{*\mathsf{T}}(\delta)Rw^*(\delta) + \nabla V^{*\mathsf{T}}(\delta)\mathcal{G}(s)(\hat{w}(\hat{\delta}_{\kappa}) - w^*(\delta)).\end{aligned} \tag{37}$$

Based on (19), (37) becomes

$$\begin{aligned}\dot{\Sigma}_{31}(t) =& -\delta^{\mathsf{T}} Q_{\delta}\delta - w^{*\mathsf{T}}(\delta)Rw^*(\delta) + 2w^{*\mathsf{T}}(\delta)R(w^*(\delta) - \hat{w}(\hat{\delta}_{\kappa}))\\ =& -\delta^{\mathsf{T}} Q_{\delta}\delta + w^{*\mathsf{T}}(\delta)Rw^*(\delta) - 2w^{*\mathsf{T}}(\delta)R\hat{w}(\hat{\delta}_{\kappa})\\ =& -\delta^{\mathsf{T}} Q_{\delta}\delta + \left(w^*(\delta) - \hat{w}(\hat{\delta}_{\kappa})\right)^{\mathsf{T}} R\left(w^*(\delta) - \hat{w}(\hat{\delta}_{\kappa})\right) - \hat{w}^{\mathsf{T}}(\hat{\delta}_{\kappa})R\hat{w}(\hat{\delta}_{\kappa})\\ =& -\delta^{\mathsf{T}} Q_{\delta}\delta + \|r\|^2\left\|w^*(\delta) - \hat{w}(\hat{\delta}_{\kappa})\right\|^2 - \|r\|^2\|\hat{w}^*(\hat{\delta}_{\kappa})\|^2.\end{aligned} \tag{38}$$

Considering $\varphi_{ic} = \hat{\varphi}_{ic} + \tilde{\varphi}_{ic}$, we get

$$\begin{aligned}\|w^*(\delta) - w(\hat{\delta}_{\kappa})\|^2 =& \left\|\left(w^*(\delta) - w^*(\hat{\delta}_{\kappa})\right) + \left(w^*(\hat{\delta}_{\kappa}) - \hat{w}(\hat{\delta}_{\kappa})\right)\right\|^2\\ \leq& 2\left\|w^*(\delta) - w^*(\hat{\delta}_{\kappa})\right\|^2 + 2\left\|w^*(\hat{\delta}_{\kappa}) - \hat{w}(\hat{\delta}_{\kappa})\right\|^2\\ \leq& \frac{1}{2}\|r^{-1}\|^2\bar{g}\left\|\nabla\sigma_c^{\mathsf{T}}(\hat{\delta}_{\kappa})\hat{\varphi}_c - \nabla\sigma_c^{\mathsf{T}}(\hat{\delta}_{\kappa})\varphi_c - \nabla\xi_c(\hat{\delta}_{\kappa})\right\|^2 + 2\mathcal{L}_w^2\|\mathbf{E}_{\kappa}(t)\|^2\\ \leq& \frac{1}{2}\|r^{-1}\|^2\bar{g}^2\| - \nabla\xi_c(\hat{\delta}_{\kappa}) - \nabla\sigma_c^{\mathsf{T}}(\hat{\delta}_{\kappa})\tilde{\varphi}_c\|^2 + 2\mathcal{L}_w^2\|\mathbf{E}_{\kappa}(t)\|^2\\ \leq& 2\mathcal{L}_w^2\|\mathbf{E}_{\kappa}(t)\|^2 + \|r^{-1}\|^2\bar{g}^2\left(\bar{\sigma}_c^2\bar{\varphi}_c^2 + \bar{\xi}_c^2\right).\end{aligned} \tag{39}$$

According to (39), we further derive from (38) as

$$\dot{\Sigma}_{31}(t) \leq -\delta^{\mathsf{T}} Q_{\delta}\delta + 2\mathcal{L}_w^2\|r\|^2\|\mathbf{E}_{\kappa}(t)\|^2 - \|r\|^2\|\hat{w}(\hat{\delta}_{\kappa})\|^2 + \underbrace{\|r^{-1}\|^2\bar{g}^2\left(\bar{\sigma}_{ic}^2\bar{\varphi}_{ic}^2 + \bar{\xi}_{ic}^2\right)}_{\Theta}. \tag{40}$$

By combining (36) and (40), we obtain

$$\dot{\Sigma}_3(t) \leq -\rho^2\lambda_{\min}(Q_{\delta})\|\delta\|^2 + (\rho^2 - 1)\lambda_{\min}(Q_{\delta})\|\delta\|^2 + 2\|r\|^2\mathcal{L}_w^2\|\mathbf{E}_{\kappa}(t)\|^2 + \Theta.$$

Therefore, if the condition (35) holds and δ lies outside the compact set

$$\Omega_{\delta} = \left\{\delta :\ \|\delta\| \leq \sqrt{\frac{\Theta}{\rho^2\lambda_{\min}(Q_{\delta})}}\right\},$$

we can find that $\dot{\Sigma}_3(t) \leq -\rho^2\lambda_{\min}(Q_{\delta})\|\delta\|^2 < 0$ for any $\delta \neq 0$.

Case 2: $\forall t = t_{s+1}$, we have

$$\begin{aligned}\Delta\Sigma_3(t) =& \Sigma_3(\hat{\delta}_{\kappa+1}) - \Sigma_3(\delta(t_{\kappa+1}^-))\\ =& \Delta\Sigma_{31}(t) + \Delta\Sigma_{32}(t).\end{aligned}$$

Noting the fact that δ and $V^*(\cdot)$ are both continuous, we derive

$$\Delta\Sigma_{31}(t) = V^*(\hat{\delta}_{\kappa+1}) - V^*(\delta(t^-_{\kappa+1})) \leq 0, \tag{41a}$$

$$\Delta\Sigma_{32}(t) = V^*(\hat{\delta}_{\kappa+1}) - V^*(\hat{\delta}_{\kappa}) \leq -\vartheta(\|\mathbf{E}_{\kappa+1}(t_\kappa)\|), \tag{41b}$$

where $\delta(t^-_{\kappa+1}) = \lim_{\Delta t \to 0} \delta(t_{\kappa+1} - \Delta t)$, $\vartheta(\cdot)$ is a class-$\mathcal{K}$ function and $\mathbf{E}_{\kappa+1}(t_\kappa) = \hat{\delta}_{\kappa+1} - \hat{\delta}_\kappa$. Based on (41), we derive $\Delta\Sigma_3(t) \leq 0$.

In the end, from the two aspects, if (35) holds, the closed-loop system is UUB. □

4 | SIMULATION RESULTS

The effectiveness of the proposed ETNOTC method is demonstrated by employing a numerical and a realistic nonlinear systems.

4.1 | Example 1

Consider the nonlinear system with uncertainties as

$$\dot{s} = \begin{bmatrix} s_2 \\ -0.5s_1^3 - 0.5s_2 \end{bmatrix} + \begin{bmatrix} 0 \\ 1 \end{bmatrix} (u + d), \tag{42}$$

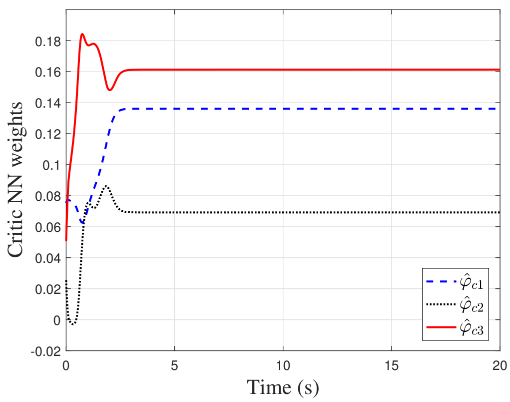

FIGURE 1 The learning process of critic NN weights.

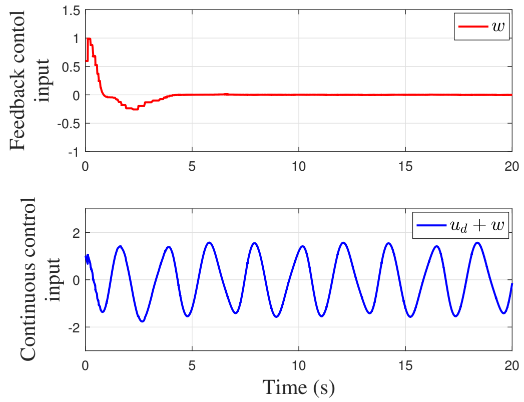

FIGURE 2 Feedback and continuous control inputs.

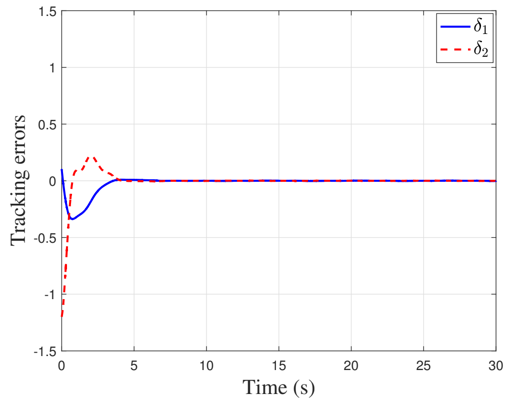

FIGURE 3 Tracking errors of system (16).

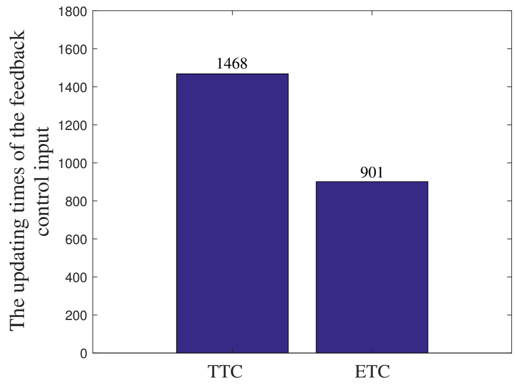

FIGURE 4 The updating times of the feedback control input.

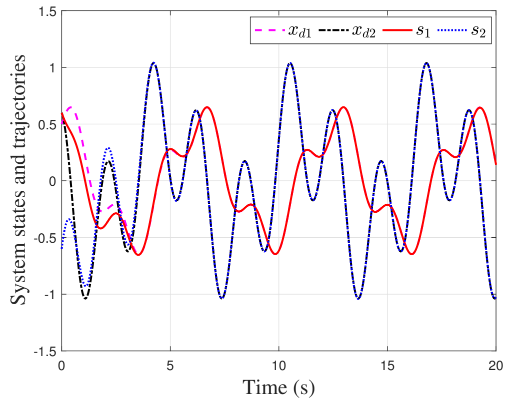

FIGURE 5 Tracking control performance.

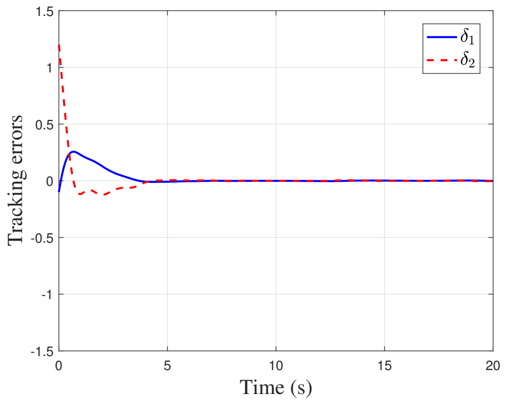

FIGURE 6 The tracking errors of system (3).

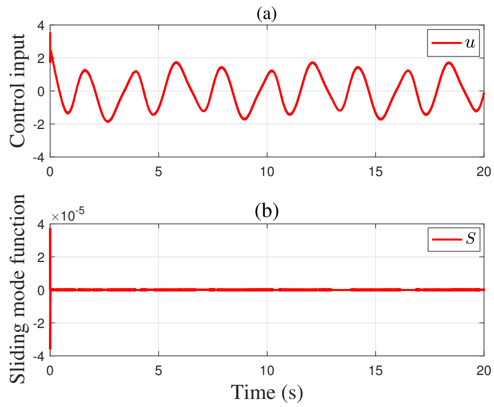

FIGURE 7 The curves of composite control input and sliding mode function.

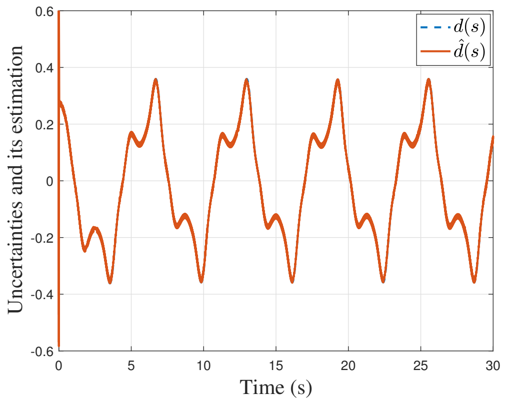

FIGURE 8 The uncertainties and its estimation.

where $s \in [s_1, s_2]^\mathsf{T}$ is the system state, $d = \sin(0.6s_1)\cos(s_2)\cos(0.6s_1)$ is the uncertainties. The reference trajectory is chosen as

$$\dot{x}_d = \begin{bmatrix} -0.5\sin(t) + 0.6\cos(3t) \\ -0.5\cos(t) - 1.8\sin(3t) \end{bmatrix}. \tag{43}$$

The feedback control input in continuous control component is designed by using ADP-based ETC control method for system (16). The parameters of the value function are set as $Q_\delta = 4I$ and $R = 0.1$. In the critic NN, the learning rate $\alpha_c = 2$, the activation function is chosen as $\sigma_c(\delta) = [\delta_1^2, \delta_1\delta_2, \delta_2^2]^\mathsf{T}$, the weight vector is defined as $\hat{\varphi}_c = [\hat{\varphi}_{c1}, \hat{\varphi}_{c2}, \hat{\varphi}_{c3}]^\mathsf{T}$. Fig. 1 displays that the weight vector of the critic NN $\hat{\varphi}_i$ finally converge to $[0.1361, 0.0691, 0.1613]^\mathsf{T}$. Fig. 2 shows the feedback control and the continuous control inputs, the feedback control input w is updated at t_κ only, and keeps unchanged during $[t_\kappa, t_{\kappa+1})$. Fig. 3 describes that the tracking errors converge to a small region of zero (SRZ) after 7s. From Fig. 4, it is found that the less updating frequency of the feedback control signal is required by using ETC than TTC mechanism, which implies that the computational and communication resources can be saved.

Then, in the discontinuous control component, the initial weight vector $\hat{\theta}$ is randomly selected within $[-1, 1]$, the RBF $h(s) = [h_1(s), h_2(s), \dots, h_{ld}(s)]^\mathsf{T}$ is chosen as

$$h_l(s) = \exp\left(\frac{-\|s - c_l\|^2}{b^2}\right), \tag{44}$$

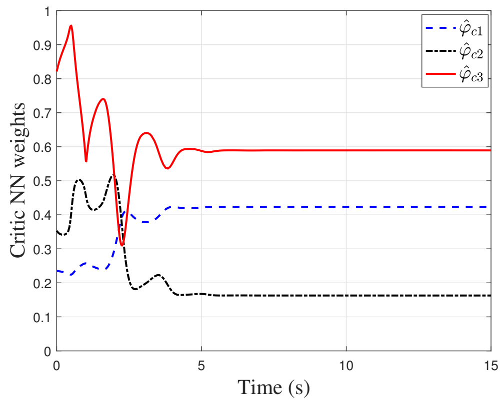

FIGURE 9 The learning process of critic NN weights.

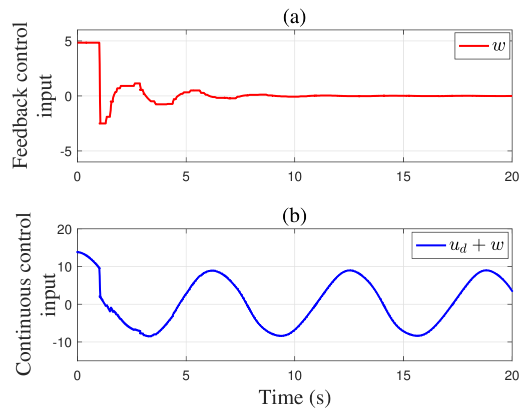

FIGURE 10 Feedback and continuous control inputs.

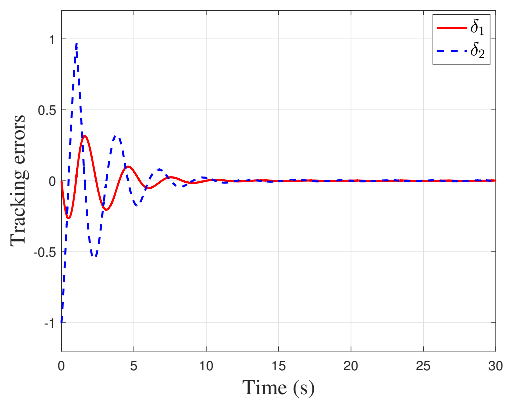

FIGURE 11 Tracking errors of system (16).

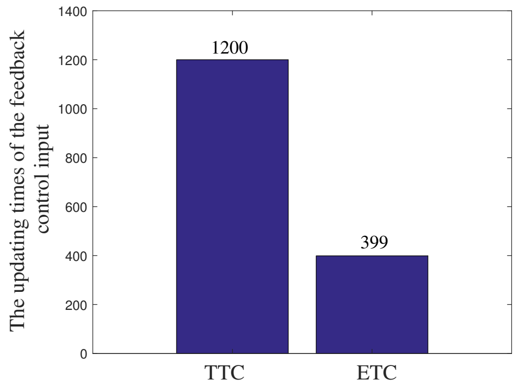

FIGURE 12 The updating times of the feedback control input.

where $l = 1, 2, \dots, l_d$, and c_l is the lth colum vector of the matrix

$$C_d = \begin{bmatrix} -3 & -2 & -1 & 0 & 1 & 2 & 3 \\ -3 & -2 & -1 & 0 & 1 & 2 & 3 \end{bmatrix}.$$

The sliding mode gain is chosen as $K = 0.02$, $A = [0, 1]$. The discontinuous control law (9) is given as $u_c = -K\text{sign}(A^{\mathsf{T}}(s) g^{\mathsf{T}}(s)S) + \hat{d}(s)$. The composite control input (4) is employed to drive the tracking error dynamics (3) for simulation. Fig 5 displays the tracking performance. As shown in Fig. 6, the the tracking errors converge to a SRZ after 7s. The curves of composite control input and sliding mode function are presented in Fig. 7. Fig. 8 shows the curves of $d(s)$ and $\hat{d}(s)$ and their difference, we can conclude that the adaptive term is effective to approximate the $d(s)$.

4.2 | Example 2

The pendulum system[48] is formulated as

$$\ddot{\theta} = -\frac{f_d}{J}\dot{\theta} - \frac{MgL}{J}\sin(\theta) + \frac{1}{J}(u + d),$$

where $\theta \in \mathbb{R}$ denotes the angle position of the pendulum, and the parameters are given in Table 1.

Let $s_1 = \theta$, $s_2 = \dot{\theta}$, we have

$$\dot{s} = \begin{bmatrix} s_2 \\ -4.9\sin(s_1) - 0.2s_2 \end{bmatrix} + \begin{bmatrix} 0 \\ 0.25 \end{bmatrix}(u + d), \tag{45}$$

TABLE 1 Parameters of the pendulum system

Parameter	J_1	L	M	g	f_d
Value	$4\ \mathrm{kg \cdot m^2}$	1.5 m	$4/3$ kg	$9.8\ \mathrm{m/s^2}$	$0.8\ \mathrm{N \cdot m \cdot s/rad}$

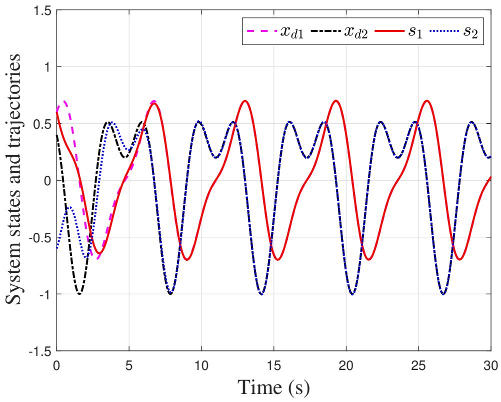

FIGURE 13 Tracking control performance.

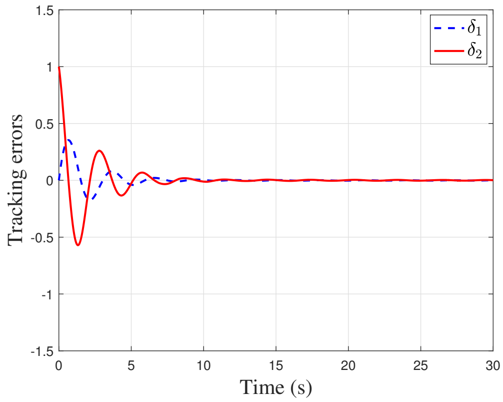

FIGURE 14 Tracking errors of system (3).

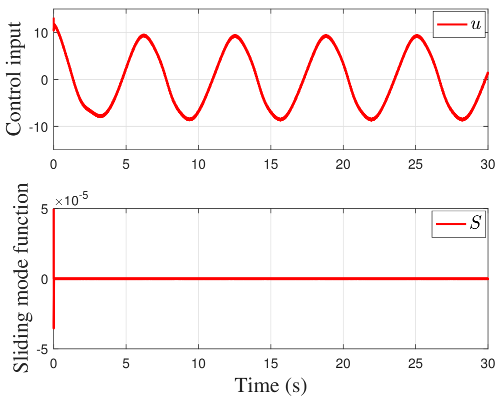

FIGURE 15 The curves of composite control input and sliding mode function.

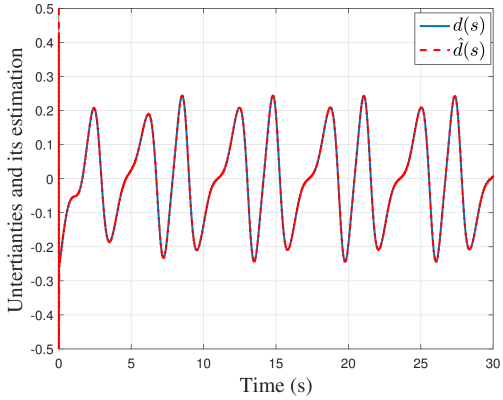

FIGURE 16 The uncertainty and its estimation.

where $s = [s_1, s_2]^{\mathrm{T}} \in \mathbb{R}^2$ is the system state, $d = \sin(s_1)\cos(s_2)\sin(s_2)$. The reference system is chosen as

$$\dot{x}_d = \begin{bmatrix} -0.6\sin(t) + 0.4\cos(2t) \\ -0.6\cos(t) - 0.8\sin(2t) \end{bmatrix}. \tag{46}$$

First, ADP-based ETC method is developed to design the feedback control input. The value function is given as (16) with $Q_\delta = 5I$ and $R = 0.05$. The structure of the critic NN is the same in Example 1. As shown in Fig. 9, the weight vector $\hat{\varphi}$ finally converges to $[0.4230, 0.1627, 0.5893]^{\mathrm{T}}$. Fig. 10 shows the feedback control and the continuous control inputs, the feedback control input w is a piecewise signal, which implies it only updated when events occur. Fig. 11 displays that the tracking errors converge to a SRZ after 15s. Fig. 12 shows the updating times of the feedback control input, the TTC and ETC methods are required 1200 and 399 times, respectively. Thus, the computation and communication resources are saved.

Then, in the discontinuous control component, $K = 0.2$, $A = [0, 1]$, and the parameters and structure of the adaptive term are selected as the same in Example 1. Furthermore, The composite control input is used to drive the tracking error dynamics.

Fig. 13 shows the tracking performance. From Fig. 14, we can find that the tracking errors converge to a SRZ after 15s. Fig. 15 displays the curves of the composite control input and the sliding mode function. According to Fig. 16, we known the adaptive term $\hat{d}(s)$ estimate $d(s)$ successfully.

5 | CONCLUSIONS

In this paper, we develop an ETNOTC method for nonlinear uncertain systems by integrating ADP and ISMC techniques. The discontinuous control input with an adaptive term is developed to eliminate the influence of uncertainties and obtain the sliding mode dynamics, this method can relax the assumption of known upper-bounded function of uncertainties, and the designed continuous control input composed of feedforward and feedback control inputs is employed to achieve the tracking task. The ADP-based feedback control input is updated only when events occur, thus the updating frequency is reduced, and the computational and communication burdens are reduced. According to Lyapunov stability theorem, we prove that the closed-loop tracking error system is asymptotically stable. Finally, the simulation results declare that the developed ETNOTC method is effective.

6 | ACKNOWLEDGMENTS

This work was supported in part by the National Natural Science Foundation of China under Grant 61971147, in part by the Guangdong Basic and Applied Basic Research Foundation under Grant 2021A1515110022, in part by the open research fund of The State Key Laboratory for Management and Control of Complex Systems under Grant 20220118, and in part by the Guangdong Province Graduate Education Innovation Project under Grant 2020JGXM040.

References

1. Liu D, Wei Q, Wang D, Yang X, Li H. *Adaptive Dynamic Programming with Applications in Optimal Control*. Springer; 2017.
2. Wang D, He H, Liu D. Adaptive critic nonlinear robust control: A survey. *IEEE Trans. Cybern.* 2017; 47(10): 3429–3451.
3. Lin M, Zhao B, Liu D. Policy gradient adaptive critic designs for model-free optimal tracking control with experience replay. *IEEE Trans. Syst. Man Cybern. Syst.* 2022;52(6):3692–3703.
4. Lu K, Liu Z, Yu H, Chen CLP, Zhang Y. Adaptive fuzzy inverse optimal fixed-time control of uncertain nonlinear systems. *IEEE Trans. Fuzzy Syst.* 2022;30(9):1–12.
5. Wang D, Liu D, Li H, Luo B, Ma H. An approximate optimal control approach for robust stabilization of a class of discrete-time nonlinear systems with uncertainties. *IEEE Trans. Syst. Man Cybern. Syst.* 2016;46(5):713–717.
6. Xue S, Luo B, Liu D, Yang Y. Constrained event-triggered H_∞ control based on adaptive dynamic programming with concurrent learning. *IEEE Trans. Syst. Man. Cybern. Syst.* 2022;52(1):357–369.
7. Xia H, Guo P. Sliding mode-based online fault compensation control for modular reconfigurable robots through adaptive dynamic programming. *Complex Intell. Syst.* 2021;8:1963–1973.
8. Li H, Yu J, Hilton C, Liu H. Adaptive sliding-mode control for nonlinear active suspension vehicle systems using T-S fuzzy approach. *IEEE Trans. Ind. Electron.* 2013;60(8):3328–3338.
9. Zhao B, Liu D, Alippi C. Sliding-mode surface-based approximate optimal control for uncertain nonlinear systems with asymptotically stable critic structure. *IEEE Trans. Cybern.* 2021;51(6):2858–2869.
10. Zhou Q, Yao D, Wang J, Wu C. Robust control of uncertain semi-Markovian jump systems using sliding mode control method. *Appl. Math. Comput.* 2016;286:72–87.

11. Liu Z, Su H, Pan S. A new adaptive sliding mode control of uncertain nonlinear systems. *Asian J. Control* 2014; 16(1):198–208.

12. Ding S, Wang J, Zheng WX. Second-order sliding mode control for nonlinear uncertain systems bounded by positive functions. *IEEE Trans. Ind. Electron.* 2015;62(9):5899–5909.

13. Cao WJ, Xu JX. Nonlinear integral-type sliding surface for both matched and unmatched uncertain systems. *IEEE Trans. Autom. Control* 2011;49(8):1355–1360.

14. Rubagotti M, Estrada A, Castanos F, Ferrara A, Fridman L. Integral sliding mode control for nonlinear systems with matched and unmatched perturbations. *IEEE Trans. Autom. Control* 2011;56(11):2699–2704.

15. Castanos F, Fridman L. Analysis and design of integral sliding manifolds for systems with unmatched perturbations. *IEEE Trans. Autom. Control* 2006;51(5):853–858.

16. Zhang H, Qu Q, Xiao G, Cui Y. Optimal guaranteed cost sliding mode control for constrained-input nonlinear systems with matched and unmatched disturbances. *IEEE Trans. Neural Netw. Learn. Syst.* 2018;29(6):2112–2126.

17. Janardhanan S, Kariwala V. Multirate-output-feedback-based LQ-optimal discrete-time sliding mode control. *IEEE Trans. Autom. Control* 2008;53(1):367–373.

18. Sun N, Niu Y, Chen B. Optimal integral sliding mode control for a class of uncertain discrete-time systems. *Optim. Control Appl. Methods* 2014;35(4):468–478.

19. Basin M, Rodriguez-Ramirez P, Ferrara A, Calderon-Alvarez D, Sliding mode optimal control for linear systems. *J. Frankl. Inst.* 2012;349(4):1350–63.

20. Poznyak A, Fridman L, Bejarano FJ. Mini-max integral sliding-mode control for multimodel linear uncertain systems. *IEEE Trans. Autom. Control* 2004;49(1):97–102.

21. Surjagade PV, Tiwari AP, Shimjith SR. Robust optimal integral sliding mode controller for total power control of large PHWRs. *IEEE Trans. Nucl. Sci.* 2018;65(7):1331–1344.

22. Das M, Mahanta C. Optimal second order sliding mode control for linear uncertain systems. *ISA Trans.* 2014;53(6):1807–1815.

23. Zhao B, Wang D, Shi G, Liu D, Li Y. Decentralized control for large-scale nonlinear systems with unknown mismatched interconnections via policy iteration. *IEEE Trans Syst Man Cybern Syst*. 2018;48(10):1725–1735.

24. Liu D, Xue S, Zhao B, Luo B, Wei Q. Adaptive dynamic programming for control: A survey and recent advances. *IEEE Trans. Syst. Man Cybern. Syst.* 2021;51(1):142–160.

25. Chen Z, Chen SZ, Chen K, Zhang Y. Constrained decoupling adaptive dynamic programming for a partially uncontrollable time-delayed model of energy systems. *Inf. Sci.* 2022;608:1352–1374.

26. Wei Q, Liu D, Liu Y, Song R. Optimal constrained self-learning battery sequential management in microgrid via adaptive dynamic programming. *IEEE/CAA J. Automa Sinica*. 2017;4(2):168–176.

27. Liu D, Wei Q. Policy iteration adaptive dynamic programming algorithm for discrete-time nonlinear systems. *IEEE Trans. Neural Netw. Learn. Syst.* 2014;25(3):621–634.

28. Vamvoudakis KG, Lewis FL. Online actor-critic algorithm to solve the continuous-time infinite horizon optimal control problem. *Automatica* 2010;46(5):878–888.

29. Vrabie D, Lewis FL. Neural network approach to continuous-time direct adaptive optimal control for partially unknown nonlinear systems. *Neural Networks* 2009;22(3):237–246.

30. Li Y, Yang G. Adaptive integral sliding mode control fault tolerant control for a class of uncertain nonlinear systems. *IET Control Theory Appl.* 2018;12(13):1864–1872.

31. Fan QY, Yang GH. Adaptive actor-critic design-based integral sliding-mode control for partially unknown nonlinear systems with input disturbances. *IEEE Trans. Neural Netw. Learn. Syst.* 2016;27(1):165–177.

32. Wang D, Liu D, Wei Q. Finite-horizon neuro-optimal tracking control for a class of discrete-time nonlinear systems using adaptive dynamic programming approach. *Neurocomputing* 2012;78:14–22.

33. Wei Q, Liu D. Adaptive dynamic programming for optimal tracking control of unknown nonlinear systems with application to coal gasification. *IEEE Trans. Autom. Sci. Eng.* 2014;11(4):1020–1036.

34. Modares H, Lewis FL. Optimal tracking control of nonlinear partially-unknown constrained-input systems using integral reinforcement learning. *Automatica* 2014;50(7):1780–1792.

35. Zhao J, Na J, Gao G. Robust tracking control of uncertain nonlinear systems with adaptive dynamic programming. *Neurocomputing* 2021;471:21–30.

36. Wang D, Mu C. Adaptive-critic-based robust trajectory tracking of uncertain dynamics and its application to a spring-mass-damper system. *IEEE Trans. Ind. Electron.* 2018;65(1):654–663.

37. Wang Z, Wei Q, Liu D. Event-triggered adaptive dynamic programming for discrete-time multi-player games. *Inf. Sci.* 2020;506:457–470.

38. Ha M, Wang D, Liu D. Event-triggered adaptive critic control design for discrete-time constrained nonlinear systems. *IEEE Trans. Syst. Man Cybern. Syst.* 2020;50(9):3158–3168.

39. Vamvoudakis KG. Event-triggered optimal adaptive control algorithm for continuous-time nonlinear systems. *IEEE/CAA J. Automa. Sinica* 2014;1(3):282–293.

40. Wang D, Mu C, Yang X, Liu D. Event-based constrained robust control of affine systems incorporating an adaptive critic mechanism. *IEEE Trans. Syst. Man Cybern. Syst.* 2017;47(7):1602–1612.

41. Zhang K, Zhang H, Jiang H, Wang Y. Near-optimal output tracking controller design for nonlinear systems using an event-driven ADP approach. *Neurocomputing* 2018;309:168–178.

42. Xue S, Luo B, Liu D, Gao Y. Event-triggered ADP for tracking control of partially unknown constrained uncertain systems. *IEEE Trans. Cybern.* 2021. https://doi.org/10.1109/TCYB.2021.3054626.

43. Lewis FL, Yesildirek A, Liu K. Multilayer neural-net robot controller with guaranteed tracking performance. *IEEE Trans. Neural Netw.* 1996;7(2):388–399.

44. Hornik K, Stinchcombe M, White H. Universal approximation of an unknown mapping and its derivatives using multilayer feedforward networks. *Neural Netw.* 1990;3(5):551–560

45. Yang X, He H. Decentralized event-triggered control for a class of nonlinear-interconnected systems using reinforcement learning. *IEEE Trans. Cybern.* 2021;51(2):635–648.

46. Zhao B, Liu D. Event-triggered decentralized tracking control of modular reconfigurable robots through adaptive dynamic programming. *IEEE Trans. Ind. Electron.* 2020;67(4):3054–3064.

47. Zhang Q, Zhao D, Zhu Y. Event-triggered H_∞ control for continuous-time nonlinear system via concurrent learning. *IEEE Trans. Syst. Man Cybern. Syst.* 2017;47(7):1071–1081.

48. Yang X, Wei Q. Adaptive critic learning for constrained optimal event-triggered control with discounted cost. *IEEE Trans. Neural Netw. Learn. Syst.* 2021;32(1):91–104.

49. Cao Z, Wang Z, Niu Y, Song J, Liu H. Sliding mode control for sampled-data systems subject to deception attacks: Handling randomly perturbed sampling periods. *IEEE Trans. Cybern.* 2022. https://doi.org/10.1109/TCYB.2022.3202486.

50. Liu C, Wang Z, Lu R, Huang T, Xu Y. Finite-time estimation for Markovian BAM neural networks with asymmetrical mode-dependent delays and inconstant measurements. *IEEE Trans. Neural Netw. Learn. Syst.* 2021. https://10.1109/TNNLS.2021.3094551.

51. Cao Z, Niu Y, Lam J, Song X. A hybrid sliding mode control scheme of Markovian jump systems via transition rates optimal design. *IEEE Trans. Syst. Man Cybern. Syst.* 2021;51(12): 7752–7763.

52. Liu C, Yang L, Tao J, Xu Y, Huang T. Set-membership filtering for complex networks with constraint communication channels. *Neural Networks* 2022;152:479–486.